Electronic Supplementary Material (ESI) for Inorganic Chemistry Frontiers.

Integration of perovskite type Bi_2MoO_6 nanosheets onto one dimensional CdS: a type-II heterostructured photocatalytic system for efficient charge separation in hydrogen evolution reaction

Rama Krishna Chava[a]*, Namgyu Son[a], Yang Soo Kim[b], Misook Kang[a]**

[a]Department of Chemistry, College of Natural Science, Yeungnam University,

280 Daehak-Ro, Gyeongsan, Gyeongbuk-38541, Republic of Korea.

[b]Korea Basic Science Institute, Gwahak-ro, Yuseong-gu, Daejeon-34133, Republic of Korea.

Corresponding Author's Address:

Dr. Rama Krishna Chava (Email: drcrkphysics@hotmail.com, rama@ynu.ac.kr)

Prof. Misook Kang (Email: mskang@ynu.ac.kr)

Department of Chemistry, College of Natural Sciences, Yeungnam University, 280 Daehak-Ro, Gyeongsan-38541, Gyeongbuk, Republic of Korea.

Contents

1. Physical characterization details: In order to get the morphological, structural and optical properties of as prepared CdS NRs, BMO NSs and CdS-Bi_2MoO_6 CSHs, several characterizations techniques were used. Field emission-scanning electron microscope (FE-SEM) images were recorded on Hitachi S-4800 instrument. Transmission electrum microscope (TEM) images were taken from Hitachi H-7600 model. High resolution TEM, Selected area electron diffraction (SAED), Scanning transmission electron microscope (STEM) images and STEM-EDS elemental mapping details were procured from FEI Titan G2 FE-TEM instrument at an operating voltage of 200 kV. Powder X-ray diffraction measurements were performed on Panalytical Xpert Pro diffractometer operating at 40 mA and 30kV. Structural information and oxidation states of pure and nanocomposite samples were determined by Raman and X-ray photoelectron spectroscopy. The specific surface area, pore-size distributions and pore diameters of all samples were analyzed by recording the adsorption-desorption isotherms at a liquid nitrogen temperature of 77 K. UV-vis absorption properties of all samples were studied by using Scinco spectrometer under the wavelength region of 300-900 nm. The electron-hole recombination rates of prepared samples were studied with the help of Scinco photoluminescence (PL) spectrometer. Time-resolved PL (TR-PL) measurements were taken on inverted-type scanning confocal microscope (MicroTime-200, Picoquant, Germany) with a 40× (air) objective. Exponential fittings for the obtained PL decays were executed using Symphotime-64 software (Ver. 2.2). Transient photocurrent and electrochemical impedance measurements were performed on IVIUMSTAT electrochemical analyzer. For this, 5 mg of sample was dispersed in DI water-ethanol mixture and then sonicated for 1 hr. After that, the sample was coated on FTO substrate with an active area of around 0.5 cm^2. Then the catalyst film was dried at 150 degrees for 6 hours. The measurements were performed on a standard three electrode system where Pt wire as counter electrode and Ag/AgCl (Saturated KCl) as reference electrode. The catalyst on FTO substrate is used as working electrode. A Xenon lamp

(150 W) with UV cutoff filter was used as light source. Electrochemical impedance (EIS) measurements were taken in a frequency range of 0.01 to 100 kHz with an AC amplitude of 5 mV. During measurements, 0.1 M Na_2SO_4 aqueous solution used as electrolyte.

2. Visible photocatalytic H_2 evolution experiments: The photocatalytic activity of all prepared photocatalyst samples were evaluated by checking the H_2 evolution reaction under visible-light irradiation using 150W Xe lamp. The reaction was carried out in a photocatalytic reactor in which 5 mg of photocatalyst sample was added to 10% lactic acid aqueous solution. After stirring and sonication for 30 min. the reactor was closed and purged with Ar gas for one hour to remove any dissolved gases. During the visible light irradiation, 200 µL of gas is sampled for each hour and analyzed with gas chromatography. The apparent quantum yield of the optimized photocatalyst sample was determine by the following equation,

$$\eta_{AQY} = 2 \times \frac{Amount\ of\ hydrogen\ gas\ molecules\ released}{Number\ of\ incident\ photons} \times 100\% \qquad \text{------- (1)}$$

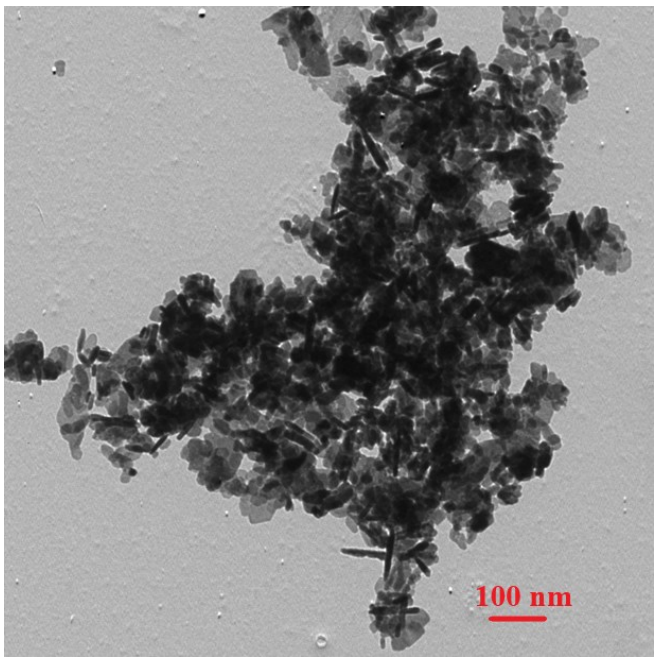

Fig. S1. TEM image of Bi_2MoO_6 nanosheets.

Table S1: Amounts of CdS, Bi and Mo precursors for the preparation of CdS-Bi_2MoO_6 CSNCs.

Samples	CdS (mg)	Bi (mg)	Mo (mg)
CB-1	20	210	50
CB-2	20	421	105
CB-3	20	842	210
BMO NSs	0	421	105

3. Control experiments: In order to validate the photocatalytic H_2 evolution activity of CB-2 sample, we have performed few control experiments related to the optimization of catalyst amount, scavengers and then volume of scavenger. Generally, the volume percent of scavenger in the reaction medium plays an important role hence the experiments with different volume percent of lactic acid were performed under identical conditions. Fig. S2 shows the effect of lactic acid content on the visible photocatalytic H_2 evolution rate of CB-2 photocatalyst sample. As seen from Fig. S2, H_2 evolution rate was increased with increasing the content of lactic acid and shown the highest rate (6.85 mmol/g/h) at 10 vol% lactic acid solution. After increasing to 20 vol% of lactic acid, hydrogen evolution rate was slightly decreased due to high viscosity and higher number of lactic acid molecules in the reaction medium which reduces the light harvesting capacity.[1] Next Fig. S3 exhibits the effect of catalyst amount on the H_2 evolution rate of CB-2 sample in 10 vol% lactic acid aqueous solution. From Fig. S3 it is concluded that the amount of 5 mg shown the best photocatalytic H_2 evolution rate, further increasing the catalyst amount beyond 5 mg displayed the lower hydrogen evolution activity. The decreased photocatalytic activity is might be due to the aggregation and lower light absorption capability of the sample. Furthermore, we have also performed few experiments to determine the best

scavenger for higher photocatalytic H_2 evolution rates. As seen from Fig. S4, the CB-2 photocatalyst sample (5 mg) is tested at 10 vol% of methanol, triethanolamine, Na_2S/Na_2SO_3 and lactic acid scavengers. Interestingly, lactic acid shown the highest hydrogen evolution rate (6.75 mmol/g/h) when compared to methanol (2.58 mmol/g/h), triethanolamine (3.1 mmol/g/h) and Na_2S/Na_2SO_3 (3.65 mmol/g/h).

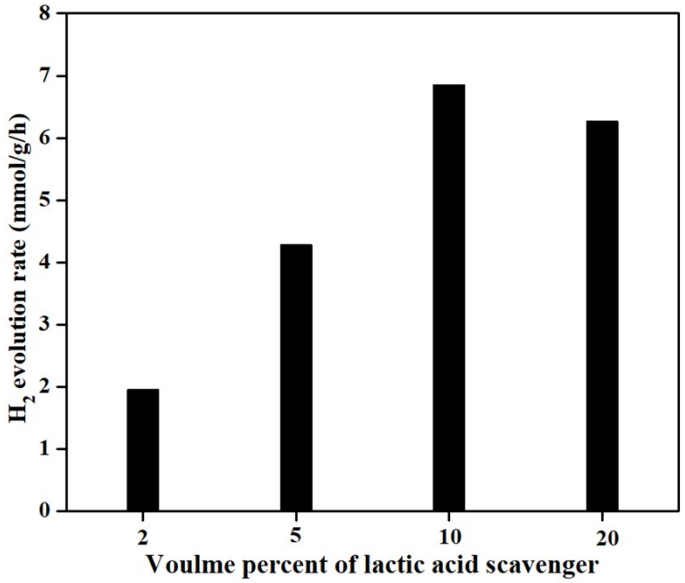

Fig. S2. Effect of lactic acid content on the H_2 evolution rate of CB-2 sample.

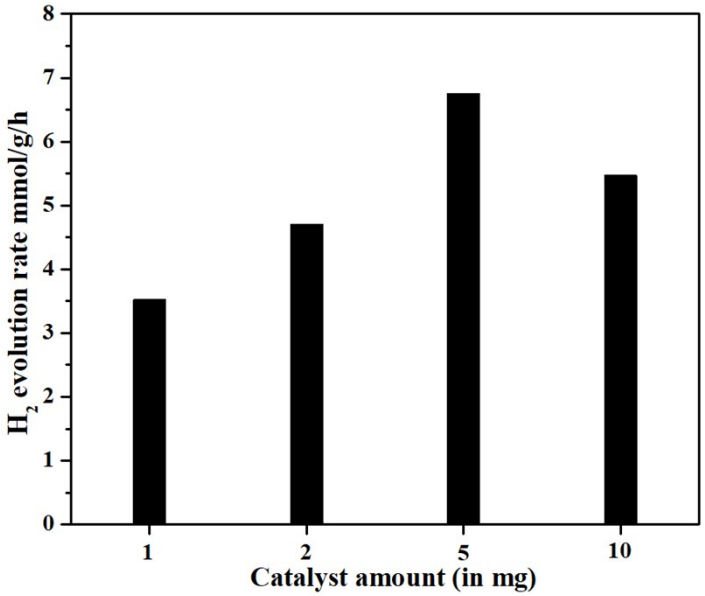

Fig. S3. Effect of CB-2 catalyst amount on visible photocatalytic H_2 evolution rate.

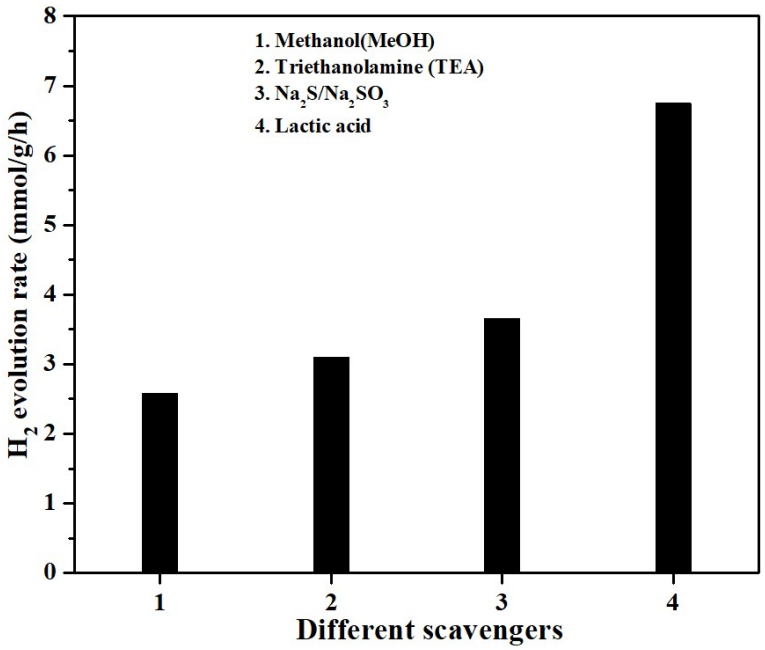

Fig. S4. Effect of different scavengers on photocatalytic H^2 evolution rate of CB-2 sample.

Table S2: Comparison of H_2 evolution activities of 1D CdS based heterostructures.

Catalyst	**Light source λ> 420 nm**	**H_2 evolution rate ($mmol.g^{-1}.h^{-1}$)**	**Quantum Efficiency**	**Ref.**
CdS/CoO_x	350 W Xe lamp	3.5	--	2
$CdS\text{-}Au/MoS_2$ 3	150 W Xe lamp	7	27.85%	
$CdS\text{-}MoS_2$ 4	300 W Xe lamp	49.80	41.37%	
$CdS\text{-}SnS_2$	150 W Xe lamp	35.65	18.45%	5
$CdS\text{-}g\text{-}C_3N_4$ 6	300 W Xe lamp	44.45	46.3%	
$CdS\text{-}CdIn_2S_4$ 7	300 W Xe lamp	0.823	1.2%	
CdS- β-NiS 8	300 W Xe lamp	793.6 $\mu mol.h^{-1}$	74.11%	
$CdS\text{-}Co(OH)_2$ 9	350 W Xe lamp	14.43	--	
CdS-Pt 10	350 W Xe lamp	1.49 $mmol.\ h^{-1}$	6.70%	
$CdS\text{-}MoS_x$	300 W Xe lamp	404 $\mu mol.h^{-1}$	--	11
$CdS\text{-}MoS_2$-graphene 12	350 W Xe lamp	621.3 $\mu mol.h^{-1}$	54.4%	
$CdS\text{-}MoS_2$ 13	300 W Xe lamp	9.73	60.3%	
CdS-ZnO 14	300 W Xe lamp	9.618	--	
$CdS\text{-}MoS_2$ 15	300 W Xe lamp	10.85	22.0%	
$CdS\text{-}g\text{-}C_3N_4\text{-}Ni(OH)_2$ 16	300 W Xe lamp	0.115	16.7%	
$CdS\text{-}CoS_2$ 17	300 W Xe lamp	5.54	10.2%	
$CdS\text{-}Bi_2MoO_6$ This work	150 W Xe lamp	6.83	5.9%	

References

1. H. Lee, D. A. Reddy, Y. J. Kim, S. Y. Chun, R. Ma, D. P. Kumar and J. K. Song and T. K. Kim, Drastic improvement of 1D-CdS solar-driven photocatalytic hydrogen evolution rate by integrating with NiFe layered double hydroxide nanosheets synthesized by liquid-phase pulsed-laser ablation, *ACS Sustainable Chem. Eng.*, 2018, **6**, 16734−16743.

2 Y. Liu, S. P. Ding, Y. Q. Shi, X. F. Liu, Z. Z. Wu, Q. Q. Jiang, T. F. Zhou, N. K. Liu and J. C. Hu, Construction of CdS/CoOx core-shell nanorods for efficient photocatalytic H_2 evolution, *Appl. Catal., B,* 2018, **234,** 109–116.

3 R. K. Chava, J. Y. Do and M. Kang, Smart Hybridization of Au Coupled CdS Nanorods with Few Layered MoS_2 Nanosheets for High Performance Photocatalytic Hydrogen Evolution Reaction, *ACS Sustainable Chem. Eng.,* 2018, **6,** 6445−6457.

4 X. –L. Yin, L. –L. Li, W. –J. Jiang, Y. Zhang, X. Zhang, L. –J. Wan and J. –S. Hu, MoS_2/CdS Nanosheets-on-Nanorod Heterostructure for Highly Efficient Photocatalytic H2 Generation under Visible Light Irradiation, *ACS Appl. Mater. Interfaces,* 2016, **8,** 15258-15266.

5 Chava, R.K.; Do, J.Y.; Kang, M.S. Enhanced Photoexcited Carrier Separation in CdS–SnS_2 Heteronanostructures: A New 1D–0D Visible-Light Photocatalytic System for the Hydrogen Evolution Reaction, *J. Mater. Chem. A* **2019**, *7*, 13614-13628.

6 T.F. Wu, P. F. Wang, J. Qian, Y.H. Ao, C. Wang and J. Hou, Noble-metal-free nickel phosphide modified CdS/C_3N_4 nanorods for dramatically enhanced photocatalytic hydrogen evolution under visible light irradiation, *Dalton Trans.*, 2017, **46**, 13793–

13801.

7 T. Wang, Y. Y. Chai, D. K. Ma, W. Chen, W. W. Zheng and S. M. Huang, Multidimensional CdS nanowire/$CdIn_2S_4$ nanosheet heterostructure for photocatalytic and photoelectrochemical applications, *Nano Res.,* 2017, **10,** 2699-2711.

8 S. D. Guan, X. L. Fu, Y. Zhang and Z. J. Peng, β-NiS modified CdS nanowires for photocatalytic H_2 evolution with exceptionally high efficiency, *Chem. Sci.,* 2018, **9,** 1574–1585.

9 X. Zhou, J. Jin, X. J. Zhu, J. Huang, J. G. Yu, W. –Y. Wong and W. –K. Wong, New $Co(OH)_2$/CdS nanowires for efficient visible light photocatalytic hydrogen production, *J. Mater. Chem. A,* 2016, **4,** 5282–5287.

10 J. Jin, J. G. Yu, G. Liu and P. K. Wong, Single crystal CdS nanowires with high visible-light photocatalytic H_2-production performance, *J. Mater. Chem. A,* 2013, **1**, 10927–10934.

11 X. L. Fu, L. Zhang, L. H. Liu, H. Li, S. G. Meng, X. G. Ye, and S. F. Chen, In situ photodeposition of MoSx on CdS nanorods as a highly efficient cocatalyst for photocatalytic hydrogen production, *J. Mater. Chem. A,* 2017, **5,** 15287–15293.

12 D. Lang, T.T. Shen and Q. J. Xiang, Roles of MoS_2 and Graphene as Cocatalysts in the Enhanced Visible-Light Photocatalytic H_2 Production Activity of Multiarmed CdS Nanorods, *ChemCatChem*, 2015, **7**, 943 – 951.

13 Y. Li, L. L. Wang, T. Cai, S. Q. Zhang, Y. T. Liu, Y. Song, X. Dong, and L. Hu, Glucose-assisted synthesize 1D/2D nearly vertical CdS/MoS_2 heterostructures for efficient photocatalytic hydrogen evolution, *Chem. Eng. J*,. 2017, **321**, 366–374.

14 S. Tso, W. –S. Li, B. –H. Wu and L. –J. Chen, Enhanced H_2 production in water splitting with CdS-ZnO core-shell nanowires, *Nano Energy*, 2018, **43**, 270-277.

15 H. F. Lin, Y. Y. Li, H. Y. Li and X. Wang, Multi-node CdS hetero-nanowires grown with defect-rich oxygen-doped MoS_2 ultrathin nanosheets for efficient visible-light photocatalytic H_2 evolution, *Nano Res.*, 2017, **10**, 1377-1392.

16 Z. P. Yan, Z. J. Sun, X. Liu, H. X. Jia and P. W. Du, Cadmium sulfide/graphitic carbon

nitride heterostructure nanowire loading with a nickel hydroxide cocatalyst for highly efficient photocatalytic hydrogen production in water under visible light, *Nanoscale*, 2016, **8**, 4748-4756.

17 P.F. Wang, Y.H. Mao, L. Li, Z.R. Shen, X. Luo, K.F. Wu, P.F. An, H.T. Wang, L. Su, Y. Li, S.H. Zhan, Unraveling the interfacial charge migration pathway at the atomic level in a highly efficient Z-scheme photocatalyst, *Angew. Chem. Int. Ed.* **2019**, *58*, 11329-11334.